

# HGTS-Former: Hierarchical HyperGraph Transformer for Multivariate Time Series Analysis

Xiao Wang, *Member, IEEE*, Hao Si, Fan Zhang, Xiaoya Zhou, Dengdi Sun, Wanli Lyu, Qingquan Yang, Jin Tang

**Abstract**—Multivariate time series analysis has long been one of the key research topics in the field of artificial intelligence. However, analyzing complex time series data remains a challenging and unresolved problem due to its high dimensionality, dynamic nature, and complex interactions among variables. Inspired by the strong structural modeling capability of hypergraphs, this paper proposes a novel hypergraph-based time series transformer backbone network, termed HGTS-Former, to address the multivariate coupling in time series data. Specifically, given the multivariate time series signal, we first normalize and embed each patch into tokens. Then, we adopt the multi-head self-attention to enhance the temporal representation of each patch. The hierarchical hypergraphs are constructed to aggregate the temporal patterns within each channel and fine-grained relations between different variables. After that, we convert the hyperedge into node features through the EdgeToNode module and adopt the feed-forward network to further enhance the output features. Extensive experiments conducted on two multivariate time series tasks and eight datasets fully validated the effectiveness of our proposed HGTS-Former. The source code will be released on [https://github.com/Event-AHU/Time\\_Series\\_Analysis](https://github.com/Event-AHU/Time_Series_Analysis).

**Index Terms**—Hypergraph Neural Network; transformer; Time Series Analysis

## I. INTRODUCTION

MULTIVARIATE time series (MTS) analysis is a critical research topic in artificial intelligence and has been widely used in nuclear fusion [1], stock prices [2]–[4], and weather conditions [5]–[7]. The main downstream tasks include forecasting, anomaly detection, classification, and interpolation. The MTS data exhibit strong spatial-temporal dependencies, such as spatial correlations between different channels at the same timestamp and temporal correlations between various timestamps. The core challenges of this task lie in the high dimensionality and complexity of multivariate time series data, the coupling between variables, as well as noise and missing values. As a result, there is currently no unified solution that can perfectly address all of the issues mentioned above.

Existing recent works usually adopt the self-attention based transformer [8]–[10] to model the time series data, as shown in Fig. 1 (a). For example, itransformer [8] treats each independent time series as a token and captures multivariate correlations through an attention mechanism. Timer [9] is

a decoder-only transformer model for univariate time series forecasting, Timer-XL [10] also utilizes decoder-only for multivariate time series forecasting, as shown in Fig. 1 (b). Time-MoE [11] is a universal decoder-only time series forecasting foundation model architecture with mixture-of-experts. Zhang et al. proposes TimesBERT [12], a BERT style foundation model. These works fully leverage the strengths of transformers in modeling global relationships, but the high-order dependencies in multivariate time series data have not been sufficiently exploited.

Some researchers resort to the Graph Neural Network (GNN) and Hypergraph to address the complex relations between different time series. For the GNN-based models, CrossGNN [13] uses a graph to build relationships between variables. TimeFilter [14] uses GNN to build connections between variables and filter different relationships through filters, as shown in Fig. 1 (c). Hi-Patch [15] aggregates multi-scale information within and between patches by building a hierarchical graph. For the hypergraph-based models, MSHyper [16] proposed a multi-scale fixed hypergraph to simulate high-order mode interactions, and Ada-MSHyper [17] further used a learnable hypergraph to model implicit group-wise interactions. HyperIMTS [18] uses hypergraphs for irregular multivariate time series forecasting. These works validated the effectiveness of hypergraphs for high-order relation mining, however, due to the utilization of message passing mechanisms, their overall performance is still limited.

Despite significant improvements having been achieved, their performance is still limited by: 1). Traditional GNN models based on ordinary graph structures can only model binary relationships (each edge connects exactly two nodes), making it difficult to capture high-order interactions. Their message-passing mechanisms are limited to local pairwise aggregation, which restricts their expressive power and generalization capability in complex relational scenarios. 2). Hypergraph neural networks for MTS data suffer from limited receptive fields due to stacking layers to capture long-range dependencies, making it difficult to model the importance differences among nodes and hyperedges, and resulting in a weak capability for capturing dynamic or heterogeneous relationships. Thus, it is natural to raise the following question: *Is it possible to design a hypergraph-based architecture with global receptive fields and adaptive attention mechanisms to overcome the limitations of both standard GNNs and existing hypergraph models for multivariate time series analysis?*

In this paper, we propose a novel hierarchical hypergraph time series transformer network to address the aforementioned question, termed HGTS-Former. The key insight of this paper

• Xiao Wang, Hao Si, Fan Zhang, Xiaoya Zhou, Dengdi Sun, Wanli Lyu, Jin Tang are with the School of Computer Science and Technology, Anhui University, Hefei 230601, China. (email: {xiaowang, tangjin}@ahu.edu.cn)

• Qingquan Yang is with the Institute of Plasma Physics, Chinese Academy of Sciences, Hefei, China. (email: yangqq@ipp.ac.cn)

\* Corresponding Author: Jin Tang

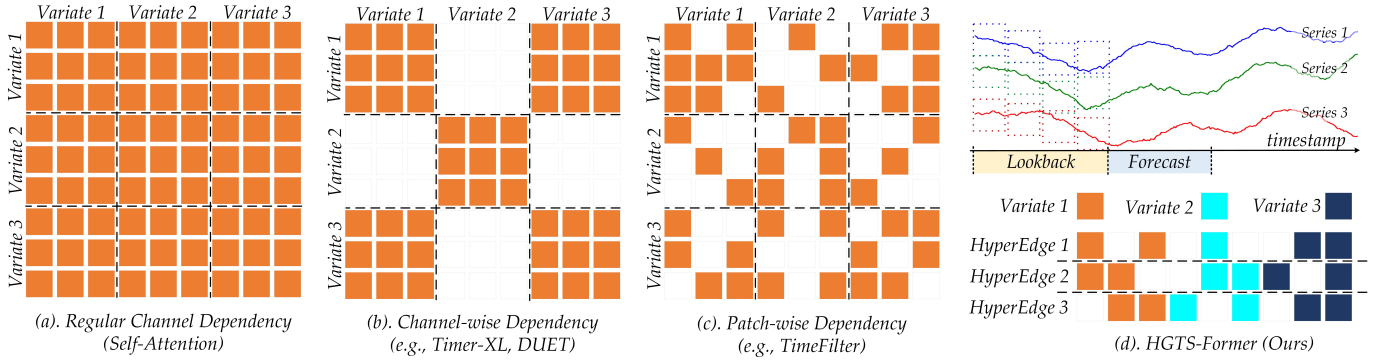


Fig. 1: Comparison between existing time series models and our newly proposed hierarchical hypergraph Transformer.

lies in our introduction of hypergraphs to model high-order dependencies in multivariate data, along with a general hierarchical attention architecture that captures both fine-grained and coarse-grained global information within and among variables, as shown in Fig. 1 (d). Given the multivariate time series data, we first standardize its distribution and map it into the shared feature space. Then, we adopt multi-head self-attention (MHSA) to enhance the temporal representation of each channel. Hierarchical hypergraph is designed to aggregate the potential temporal patterns within variables and fine-grained soft channel correlations between variables. Then, the hyperedge information is converted into node features via the Edge2Node module and fed into the feed-forward networks to output the final representation. An overview of our proposed HGTS-Former is illustrated in Fig. 2.

To sum up, the main contributions of this paper can be summarized as follows:

- 1). We propose a novel hierarchical hypergraph transformer, termed HGTS-Former, to effectively model the multivariate time series data in both fine-grained and coarse-grained manner.
- 2). We propose the intra- and inter-hypergraph attention aggregation layers to flexibly extract and model high-order and global dependencies of various time series.
- 3). Extensive experiments on two multivariate time series tasks, eight datasets, including long-term forecasting and imputation, fully validated the effectiveness of our proposed hypergraph transformer networks.

*The rest of this paper is organized as follows:* In section II, we introduce the most relevant related works from self-attention and transformer, time series analysis, and hypergraph neural networks. In section III, we dive into the details of our proposed approach, with a focus on the review of graph and hypergraph, overview, input encoding, detailed network architectures, and loss function. In section IV, we conduct the experiments to validate the effectiveness of our model on two multivariate time series tasks. In section V, we conclude this paper and propose possible research directions for future work.

## II. RELATED WORKS

In this section, we introduce the related works with a focus on Self-Attention and transformer, Time Series Analysis,

Hypergraph Neural Network. More related works can be found in the following surveys [19] and paper list <sup>1</sup>.

### A. Self-Attention and Transformer

The transformer architecture [20] has brought about a paradigm shift in various fields [21]–[24]. By leveraging the self-attention mechanism, it overcomes the limitations of traditional recurrent neural networks (RNNs) in handling long-range dependencies. Self-attention allows the model to compute the attention weights between all positions in the input sequence, enabling it to capture global information more effectively. Since its advent, numerous transformer-based models have emerged. For example, BERT [25] has shown remarkable performance in natural language processing (NLP) tasks. In the computer vision domain, Vision transformer (ViT) [26] extends the transformer architecture to image classification by treating image patches as sequence elements. With the success of transformers in NLP and computer vision, many transformer-based time series models have emerged in the field of time series analysis, such as itransformer [8], PatchTST [27].

Transformers have been extensively applied to time series forecasting. Initial transformer-based forecasters primarily focused on long-term forecasting [28], [29], with efforts to reduce the complexity of the original attention mechanism through designs such as Fourier-enhanced structures [30], and pyramid attention modules [31], though most relied on point-wise attention and overlooked the potential of patches. Afterwards, the field has seen a shift towards pre-trained large models [32]–[34], with decoder-only transformers gaining attention. Building on these advancements, Timer-XL [10] emerges as a causal decoder-only transformer for unified time series forecasting, generalizing next token prediction to multivariate scenarios.

### B. Time Series Analysis

Multivariate time series forecasting is a complex task that aims to predict future values of multiple variables considering their interdependencies. Traditional methods such as the autoregressive integrated moving average (ARIMA) model

<sup>1</sup>[https://github.com/Event-AHU/Time\\_Series\\_Analysis](https://github.com/Event-AHU/Time_Series_Analysis)

and its extensions for multiple variables [35]–[37] have been widely used. However, these linear models often struggle to capture non-linear relationships and complex temporal patterns in the data. With the development of machine learning and deep learning, deep neural network-based models like Stacked Long Short-Term Memory (S-LSTM) [38] have been proposed to improve the accuracy of multivariate time series forecasting.

Channel Independent (CI) [27], [39], [40] approaches in time series analysis treat each variable in a multivariate time series independently. Within the PatchTST [27] framework, each univariate series from a multivariate time series is fed independently into the transformer backbone, with each generating its own attention maps and prediction results while sharing the same transformer weights. In contrast, Channel Dependent (CD) [13], [41], [42] strategies focus on capturing the dependencies between variables. CrossGNN [13] designs a Cross-Variable GNN that distinguishes between homogeneous and heterogeneous relationships among variables, selecting nodes with high correlation scores as positive neighbors and those with low scores as negative neighbors.

Recent efforts [43]–[45] have sought to leverage both the advantages of CI and CD strategies. For instance, Chen et al. [43] introduces a Channel Clustering Module (CCM) that dynamically groups channels with intrinsic similarities, utilizes cluster information instead of individual channel identities, and employs a cluster-aware Feed Forward mechanism to integrate the strengths of both strategies. However, their coarse-grained designs are often insufficient to capture the dynamic and evolving nature of interactions. To address this limitation, TimeFilter [14] aims to customize the required dependency relationships for each segment period through a fine-grained filtering mechanism. Nonetheless, TimeFilter’s reliance on standard pairwise graphs and indirect inter-variable modeling fundamentally limits its capacity to capture complex higher-order group dependencies and express nuanced channel-wise correlations.

### C. Hypergraph Neural Network

Hypergraph neural networks (HGNNs), serving as a generalized variant of GNNs, have been employed across diverse domains. Hypergraphs allow hyperedges to connect more than two vertices, enabling them to represent more complex relationships. Within the realms of machine learning and deep learning, HGNNs [46]–[48] have been developed to handle data with such sophisticated interconnections. Specifically, GroupNet [48] constructs a trainable multiscale hypergraph to capture both pairwise and group-wise interactions across multiple group sizes, and employs a three-element representation format for end-to-end learning and explicit relational reasoning in multi-agent trajectory prediction. HyperGCN [49] laid the foundation for applying hypergraph convolution in relational data, demonstrating that hypergraphs can better model group-wise correlations compared to traditional GNNs. This insight was extended to time series forecasting, where MSHyper [16] proposed a multi-scale hypergraph transformer to model high-order pattern interactions, using rule-based hyperedges to connect time steps with inherent periodicity. However, such

methods rely on predefined hypergraph structures, which may fail to capture implicit temporal correlations and introduce noise in complex scenarios. Notably, Ada-MSHyper [17] further advances this direction by proposing an adaptive multi-scale hypergraph transformer that models implicit group-wise interactions across scales and differentiates temporal variations, avoiding over-reliance on fixed structures.

However, most of these studies rely on traditional HGNN methods, which may have limitations in handling large-scale data and complex temporal patterns. In our work, we introduce a novel approach that uses a hierarchical hypergraph structure in combination with a transformer-like architecture to better model the fine-grained dynamic channel correlations and aggregate latent temporal patterns in time series data, without resorting to traditional HGNNs methods.

## III. OUR PROPOSED APPROACH

### A. Preliminaries: Graph and HyperGraph

Graph is one of the most basic data structures. A graph is usually defined as  $G = \{V, E\}$ , where  $V = \{V_1, V_2, V_3, \dots, V_n\}$  is the vertex set, where  $n$  is the number of vertices,  $E = \{e_1, e_2, e_3, \dots, e_m\}$  is the edge set, where  $m$  is the number of edges, and each edge can only connect two vertices. The relationship between nodes can be represented as an adjacency matrix  $A \in R^{N \times N}$ , where  $N$  is the number of nodes. The adjacency matrix  $A$  can be expressed as below:

$$A_{ij} = \begin{cases} 1, & V_i, V_j \in e_{ij} \\ 0, & V_i, V_j \notin e_{ij} \end{cases} \quad (1)$$

Compared with hypergraphs, ordinary graphs have obvious limitations in modeling high-order relationships. The fundamental reason is that each edge of a graph can only connect two nodes, while the hyperedge of a hypergraph can connect two or more nodes, thereby improving the ability to represent high-order interactions. The topological relationship of a hypergraph can be represented as an incidence matrix  $H \in R^{N \times M}$ , where  $N$  represents the number of nodes and  $M$  represents the number of hyperedges. The matrix  $H$  is shown in the following Eq. 2:

$$H_{mn} = \begin{cases} 1, & V_n \in e_m \\ 0, & V_n \notin e_m \end{cases} \quad (2)$$

### B. Overview

Fig. 2 shows the structural framework of HGTS-Former. Its core innovation is the use of a two-layer hypergraph structure to aggregate potential temporal patterns and model fine-grained dynamic channel correlations. Specifically, the model first standardizes the distribution of time series through the InstanceNorm layer, and then uses the Embedding layer to divide the patches and map them to the shared feature space. On this basis, we use the MHSA module to enhance the temporal representation of each patch. In addition, we also use hierarchical hypergraphs to complete the aggregation of potential temporal patterns within variables and fine-grained soft channel correlations between variables. After that, the model converts the hyperedge information into node features

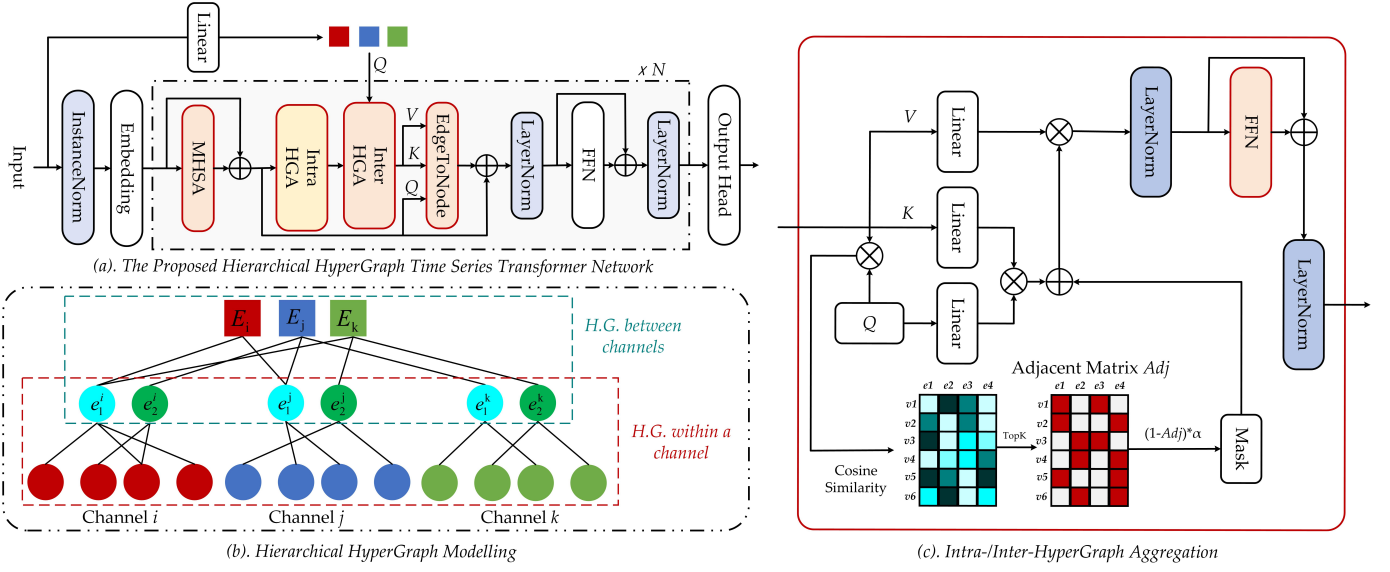


Fig. 2: An overview of our proposed HyperGraph Time Series Transformer. We use the Intra-/Inter-HGA module to construct the hierarchical hypergraph in (b) and perform fine-grained aggregation within variables and coarse-grained aggregation between variables.

through the EdgeToNode module, and finally inputs the processed features into the feedforward neural network and the downstream task output head to obtain the final prediction results. It is worth noting that in the aggregation process of the hypergraph, we only use sparsity and transformer [20] instead of traditional HGNNs [50].

### C. Input Representation

As shown in Fig. 2, we use the InstanceNorm layer to unify the distribution of the time series  $X \in R^{B \times C \times L}$ , and then use the Embedding layer to divide the  $X$  of length  $L$  into non-overlapping patches  $X_p \in R^{B \times C \times N \times P}$ , where  $B$  is the batchsize,  $P$  is the length of each patch,  $C$  is the number of variables, and  $N = \lfloor \frac{L}{P} \rfloor$  is the number of patch. Then each patch will be mapped to the shared feature space  $X_p \in R^{B \times C \times N \times D}$ ,

$$X_{norm} = \text{InstanceNorm}(X), \quad (3)$$

$$X_p = \text{Embedding}(X_{norm}), \quad (4)$$

where  $D$  is the feature dimension.

### D. Hierarchical HyperGraph Times Series Blocks

In order to obtain a more robust feature representation, we use a multi-head self-attention (MHSA) mechanism to enhance the temporal pattern representation of each patch in each variable and capture the complex temporal dependencies of different patches of the same variable. Since the self-attention mechanism is permutation invariant, but the time series is ordered in the temporal dimension, in order to reflect the position relationship of each patch token in the time series, we use RoPE [51], which has been proven to be effective in

Timer-XL [10], to inject position information into patch token. The process is as follows:

$$\hat{X}_p = W_P \text{MHSA}(W_Q X_p, W_K X_p, W_V X_p) + X_p \quad (5)$$

where  $W_Q, W_K, W_V$  are linear layer parameters,  $W_P$  is the projection layer parameter and  $\hat{X}_p \in R^{BC \times N \times D}$  is the enhanced node feature.

Hi-Patch [15] is used for irregular multivariate time series prediction (IMTS). It aggregates fine-grained information within a patch through the Intra-Patch Graph Layer and aggregates information between different patches through the Inter-Patch Graph Layer. Through these two modules, local to global aggregation is completed. Inspired by it, we use hierarchical hypergraphs to model complex relationships within a single variable and between multiple variables. As shown in Fig. 2 (b), we leverage the H.G. within a channel to capture latent temporal patterns within a single variable and use the H.G. between channels to capture the dynamic dependencies between multiple variables.

• **Intra-HyperGraph.** Fixelle et al. [52] innovatively proposed a hypergraph vision transformer, using transformers to complete the process from nodes to hyperedges and from hyperedges to nodes. Inspired by it, we propose the Intra-/Inter-HyperGraph Aggregation Module to complete the construction of hierarchical hypergraphs. As shown in Fig. 2 (c), for Intra-HyperGraph, inspired by TQNet [53], we use a learnable query  $Q \in R^{E \times D}$  as a potential pattern to capture the potential distribution between the same variables in an adaptive way, where  $E$  is the number of hyperedges and  $D$  is the feature dimension. Then, we calculate the cosine similarity between the node and  $Q$ , and then obtain a confidence matrix  $M_{conf} \in R^{BC \times E \times N}$  through the sigmoid activation function. We sample and generate the adjacency matrix  $Adj \in R^{BC \times E \times N}$  of the Intra-HyperGraph through



the TOPK method, and finally obtain the  $Mask \in R^{BC \times E \times N}$  matrix through the Adj matrix. The process is as follows:

$$M_{conf} = \sigma(Q\hat{X}_P^T) \quad (6)$$

$$Adj = TOPK(M_{conf}) \quad (7)$$

$$Mask = (1 - Adj) \times \alpha \quad (8)$$

where  $\sigma(\cdot)$  operation is the sigmoid function,  $\hat{X}_P^T \in R^{BC \times N \times D}$  is the transpose of  $\hat{X}_P \in R^{BC \times D \times N}$ ,  $\alpha$  is a hyperparameter that reduces the influence of non-edge nodes on the aggregation process.

Finally, we use the cross attention mechanism and  $Mask$  to complete the aggregation of nodes to hyperedges. Unlike traditional HGNNs, when performing aggregation, the attention mechanism calculates the contribution of each node to each hyperedge. This method can avoid aggregating unnecessary redundant information, and this process is completely adaptive. After the aggregation is completed, the aggregated hyperedge features are sent to the LayerNorm layer and the feedforward neural network, and finally output through the skip connection and LayerNorm layer. The aggregation process is shown in the following equations:

$$X_{intra} = softmax(\frac{(W_Q Q)(W_K \hat{X}_P)^T}{\sqrt{d_k}} + Mask)W_V \hat{X}_P \quad (9)$$

$$\hat{X}_{intra} = LN(FFN(LN(X_{intra}))) + X_{intra} \quad (10)$$

where  $Q \in R^{E \times D}$  is a set of learnable queries,  $\hat{X}_P \in R^{BC \times N \times D}$  is the node features after MHSA enhancement,  $Mask \in R^{BC \times E \times N}$  is the attention mechanism mask,  $W_Q, W_K, W_V$  are the linear layer parameters, and  $d_k$  is the scale factor used for scaling.

In this way, we complete the construction of Intra-HyperGraph and aggregate node information with similar temporal patterns into hyperedge  $e_i^j$  as shown in Fig. 2(b), where  $i, j$  refer to the  $i$ th hyperedge of the  $j$ th variable.

• **Inter-HyperGraph.** After completing the construction of the Intra-HyperGraph of the variable, we obtain the H.G. within a channel as shown in Fig. 2(b). For the Inter-HyperGraph, we regard the hyperedges after the Intra-HyperGraph as nodes of the Inter-HyperGraph, so we reshape  $\hat{X}_{intra} \in R^{BC \times E \times D}$  into  $\tilde{X}_{intra} \in R^{B \times CE \times D}$  and reshape  $\hat{X}_p \in R^{BC \times N \times D}$  into  $\tilde{X}_p \in R^{B \times CN \times D}$ , where  $C$  is the number of channels,  $E$  is the hyperedge number of Intra-HyperGraph.

Different from the learnable query of Intra-HyperGraph, we use linear layers to map the original time series  $X \in R^{B \times C \times L}$  to obtain queries  $Q_G \in R^{B \times C \times D}$  with global information, which we use to guide the generation of Inter-HyperGraph and the aggregation of nodes to hyperedges. In this way, we can capture the fine-grained dynamic correlation between variables. The aggregation process is the same as Intra-HyperGraph.

$$Q_G = Linear(X) \quad (11)$$

$$X_{inter} = softmax(\frac{(W_Q Q_G)(W_K \tilde{X}_{intra})^T}{\sqrt{d_k}} + Mask)W_V \tilde{X}_{intra} \quad (12)$$

$$\hat{X}_{inter} = LN(FFN(LN(X_{inter}))) + X_{inter} \quad (13)$$

where  $\hat{X}_{inter} \in R^{B \times C \times D}$ ,  $W_Q, W_K, W_V$  are the linear layer parameters, and  $d_k$  is a scale factor.

• **EdgeToNode.** As shown in Fig. 2, we use the Intra-HGA module and the Inter-HGA module to complete the construction of the hierarchical hypergraph, and use the Intra-HGA module to aggregate the potential temporal patterns within the variables and use the Inter-HGA module to adaptively capture the fine-grained dynamic correlations between variables. After hierarchical aggregation, we leverage the EdgeToNode module to complete the process of hyperedge to node. Its process is as follows:

$$X_{node} = W_P softmax(\frac{(W_Q \tilde{X}_p)(W_K \hat{X}_{inter})^T}{\sqrt{d_k}})W_V \hat{X}_{inter} + \tilde{X}_p \quad (14)$$

where  $X_{node} \in R^{B \times CN \times D}$  and  $W_P$  are the projection layer parameters. Then we feed  $X_{node}$  into the feedforward neural network, the process is as follows:

$$\hat{X}_{node} = LN(FFN(LN(X_{node}))) + X_{node} \quad (15)$$

where  $\hat{X}_{node} \in R^{B \times CN \times D}$ .

#### E. Loss Function

For different downstream tasks, such as forecasting, imputation, we can define different output heads. For forecasting and imputation tasks, we use the linear layer as the output head, and the loss function is the MSE loss function.

$$\hat{Y} = RevIN(Reshape(W_O \hat{X}_{node})) \quad (16)$$

where  $\hat{Y} \in R^{B \times C \times L}$  is the final output,  $W_O$  are linear parameters and  $RevIN(\cdot)$  operation is reverse normalization.

The loss function is as follows:

$$L_{MSE} = \frac{1}{T} \sum_{i=1}^T (Y - \hat{Y})^2 \quad (17)$$

where  $T$  is the forecasting or imputation Length,  $Y \in R^{B \times C \times L}$  is the ground truth.

#### F. Difference with Existing Hypergraph-based Models

HyperMixer [54] dynamically constructs hypergraph structures adapted to different temporal phases, which incorporates a router layer and multiple experts to identify distinct time periods and generate corresponding specialized hypergraphs. This design allows for flexible capture of high-order channel interactions and time-varying patterns. Nevertheless, it relies on HGNNs-based message passing with a two-phase mechanism to encode the hypergraph. In addition, Ada-MSHyper [17] is also based on HGNNs. Ada-MSHyper constructs hypergraphs through an adaptive hypergraph learning module that generates scale-specific incidence matrices by calculating similarity between node embeddings and hyper-edge embeddings, while its main limitation is that the features extracted by the multi-scale feature extraction module may contain redundant information. Although HyperIMTS [18] utilizes a transformer to complete the message passing process of the hypergraph, its hypergraph structure is fixed. In

TABLE I: Full multivariate forecasting results: we conduct rolling forecast with a single model trained on each dataset (lookback length is 672) and accomplish four forecast lengths in {96, 192, 336, 720}.

		HGTS-Former (Ours)		Timer-XL (2025)		Timer (2024c)		UniTST (2024a)		itransformer (2023)		DLinear (2023)		PatchTST (2022)		TimesNet (2022)		Stationary (2022b)	
		MSE	MAE	MSE	MAE	MSE	MAE	MSE	MAE	MSE	MAE	MSE	MAE	MSE	MAE	MSE	MAE	MSE	MAE
ETTh1	96	0.375	<b>0.393</b>	<b>0.364</b>	<u>0.397</u>	0.371	0.404	0.379	0.415	0.387	0.418	<u>0.369</u>	0.400	0.373	0.403	0.452	0.463	0.452	0.478
	192	<b>0.405</b>	<b>0.414</b>	<b>0.405</b>	0.424	<u>0.407</u>	0.429	0.415	0.438	0.416	0.437	<b>0.405</b>	<u>0.422</u>	<b>0.405</b>	0.425	0.474	0.477	0.484	0.510
	336	<b>0.417</b>	<b>0.424</b>	0.427	<u>0.439</u>	0.434	0.445	0.440	0.454	0.434	0.450	0.435	0.445	<u>0.423</u>	0.440	0.493	0.489	0.511	0.522
	720	<b>0.434</b>	<b>0.443</b>	0.439	<u>0.459</u>	0.461	0.466	0.482	0.482	0.447	0.473	0.493	0.508	<u>0.445</u>	0.471	0.560	0.534	0.571	0.543
	Avg	<b>0.408</b>	<b>0.419</b>	<u>0.409</u>	<u>0.430</u>	0.418	0.436	0.429	0.447	0.421	0.445	0.426	0.444	0.412	0.435	0.495	0.491	0.505	0.513
ETTh2	96	0.289	<b>0.343</b>	<b>0.277</b>	<b>0.343</b>	<u>0.285</u>	<u>0.344</u>	0.343	0.398	0.304	0.362	0.305	0.371	0.289	0.347	0.340	0.374	0.348	0.403
	192	<b>0.346</b>	<b>0.381</b>	<u>0.348</u>	<u>0.391</u>	0.365	0.400	0.376	0.420	0.372	0.407	0.412	0.439	0.360	0.393	0.402	0.414	0.408	0.448
	336	<b>0.367</b>	<b>0.399</b>	<u>0.375</u>	<u>0.418</u>	0.412	0.440	0.399	0.435	0.418	0.440	0.527	0.508	0.389	0.420	0.452	0.452	0.424	0.457
	720	<b>0.385</b>	<b>0.421</b>	0.409	0.458	0.468	0.487	0.419	0.457	0.463	0.476	0.830	0.653	<u>0.398</u>	<u>0.440</u>	0.462	0.468	0.448	0.476
	Avg	<b>0.347</b>	<b>0.386</b>	<u>0.352</u>	0.402	0.382	0.418	0.384	0.428	0.389	0.421	0.518	0.493	0.359	<u>0.400</u>	0.414	0.427	0.407	0.446
ETTm1	96	0.291	<b>0.336</b>	0.290	0.341	<b>0.281</b>	<u>0.338</u>	0.289	0.348	0.311	0.365	0.307	0.350	<u>0.285</u>	0.346	0.338	0.387	0.414	0.414
	192	0.335	<b>0.362</b>	0.337	0.369	<u>0.330</u>	<u>0.368</u>	0.332	0.375	0.353	0.390	0.337	<u>0.368</u>	<b>0.329</b>	0.372	0.371	0.375	0.524	0.482
	336	<u>0.365</u>	<b>0.382</b>	0.374	0.392	0.367	0.393	<u>0.365</u>	<u>0.397</u>	0.387	0.411	0.366	<u>0.387</u>	<b>0.363</b>	0.394	0.410	0.411	0.541	0.497
	720	<b>0.419</b>	<b>0.414</b>	0.437	0.428	0.432	0.433	<u>0.421</u>	0.431	0.452	0.445	<b>0.419</b>	0.419	<u>0.421</u>	0.426	0.478	0.450	0.578	0.509
	Avg	0.353	<b>0.374</b>	0.359	0.382	<u>0.352</u>	0.383	<u>0.352</u>	0.388	0.376	0.403	0.357	<u>0.381</u>	<b>0.349</b>	0.385	0.399	0.406	0.514	0.475
ETTm2	96	0.173	<b>0.254</b>	0.175	<u>0.257</u>	0.175	<u>0.257</u>	0.171	0.260	0.183	0.272	<b>0.167</b>	0.263	0.172	0.259	0.187	0.267	0.237	0.306
	192	0.234	<u>0.295</u>	0.242	0.301	0.239	0.301	<b>0.228</b>	<b>0.230</b>	0.250	0.315	<u>0.230</u>	0.311	0.233	0.299	0.249	0.309	0.330	0.387
	336	0.289	<b>0.331</b>	0.293	0.337	0.293	0.342	<u>0.282</u>	<u>0.336</u>	0.311	0.356	0.298	0.361	<b>0.280</b>	<b>0.331</b>	0.321	0.351	0.404	0.424
	720	<u>0.372</u>	<b>0.384</b>	0.376	0.390	0.392	0.407	0.380	0.398	0.417	0.419	0.432	0.446	<b>0.357</b>	<b>0.382</b>	0.497	0.403	0.525	0.486
	Avg	0.267	<u>0.316</u>	0.271	0.322	0.275	0.327	<u>0.265</u>	<b>0.306</b>	0.290	0.340	0.282	0.345	<b>0.261</b>	0.318	0.314	0.333	0.374	0.401
ECL	96	<u>0.128</u>	<u>0.220</u>	<b>0.127</b>	<b>0.219</b>	0.129	0.221	0.130	0.225	0.133	0.229	0.138	0.238	0.132	0.232	0.184	0.288	0.185	0.287
	192	<u>0.147</u>	<u>0.239</u>	<b>0.145</b>	<b>0.236</b>	0.148	0.239	0.150	0.244	0.158	0.258	0.152	0.251	0.151	0.250	0.192	0.295	0.282	0.368
	336	<u>0.163</u>	<u>0.256</u>	<b>0.159</b>	<b>0.252</b>	0.164	0.256	0.166	0.262	0.168	0.262	0.167	0.268	0.171	0.272	0.200	0.303	0.289	0.377
	720	<u>0.200</u>	<u>0.287</u>	<b>0.187</b>	<b>0.277</b>	0.201	0.289	0.206	0.297	0.205	0.294	0.203	0.302	0.222	0.318	0.228	0.325	0.305	0.399
	Avg	<u>0.159</u>	<u>0.250</u>	<b>0.155</b>	<b>0.246</b>	0.161	0.251	0.163	0.257	0.164	0.258	0.165	0.265	0.169	0.268	0.201	0.303	0.265	0.358
Traffic	96	<u>0.347</u>	0.244	<b>0.340</b>	<b>0.238</b>	0.348	0.240	0.359	0.250	0.353	0.259	0.399	0.285	0.359	0.255	0.593	0.315	0.610	0.322
	192	<u>0.367</u>	0.253	<b>0.360</b>	<b>0.247</b>	0.369	0.250	0.373	0.257	0.373	0.267	0.409	0.290	0.377	0.265	0.596	0.317	0.626	0.346
	336	<u>0.382</u>	0.261	<b>0.377</b>	<b>0.256</b>	0.388	0.260	0.386	0.265	0.386	0.275	0.422	0.297	0.393	0.276	0.600	0.319	0.633	0.352
	720	0.419	<u>0.282</u>	<b>0.418</b>	<b>0.279</b>	0.431	0.285	0.421	0.286	0.425	0.296	0.461	0.319	0.436	0.305	0.619	0.335	0.651	0.366
	Avg	<u>0.379</u>	0.260	<b>0.374</b>	<b>0.255</b>	0.384	<u>0.259</u>	0.385	0.265	<u>0.384</u>	0.274	0.423	0.298	0.391	0.275	0.602	0.322	0.630	0.347
Weather	96	0.155	<b>0.200</b>	0.157	0.205	0.151	0.202	0.152	0.206	0.174	0.225	0.169	0.229	<b>0.149</b>	0.202	0.169	0.228	0.185	0.241
	192	0.200	<b>0.242</b>	0.206	0.250	<u>0.196</u>	0.245	0.198	0.249	0.227	0.268	0.211	0.268	<b>0.194</b>	0.245	0.222	0.269	0.286	0.325
	336	<u>0.249</u>	<b>0.279</b>	0.259	0.291	<u>0.249</u>	0.288	0.251	0.291	0.290	0.309	0.258	0.306	<b>0.244</b>	<u>0.285</u>	0.290	0.310	0.323	0.347
	720	<b>0.316</b>	<b>0.325</b>	0.337	0.344	0.330	0.344	0.322	0.340	0.374	0.360	0.320	0.362	<u>0.317</u>	<u>0.338</u>	0.376	0.364	0.436	0.401
	Avg	<u>0.230</u>	<u>0.262</u>	0.240	0.273	0.232	0.270	0.231	0.272	0.266	0.291	0.239	0.291	<b>0.226</b>	<u>0.268</u>	0.264	0.293	0.308	0.329
Solar-Energy	96	<b>0.158</b>	<b>0.204</b>	<u>0.162</u>	<u>0.221</u>	0.212	0.230	0.190	0.240	0.183	0.265	0.193	0.258	0.168	0.237	0.180	0.272	0.199	0.290
	192	<b>0.178</b>	<b>0.219</b>	<u>0.187</u>	<u>0.239</u>	0.232	0.246	0.223	0.264	0.205	0.283	0.214	0.274	0.189	0.257	0.199	0.286	0.243	0.307
	336	<b>0.197</b>	<b>0.234</b>	<u>0.205</u>	<u>0.255</u>	0.237	<u>0.253</u>	0.250	0.283	0.224	0.299	0.233	0.291	0.212	0.277	0.220	0.301	0.264	0.322
	720	<b>0.228</b>	<b>0.259</b>	<u>0.238</u>	<u>0.279</u>	0.252	<u>0.266</u>	0.292	0.311	0.239	0.316	0.246	0.307	0.240	0.305	0.251	0.321	0.310	0.339
	Avg	<b>0.190</b>	<b>0.229</b>	<u>0.198</u>	<u>0.249</u>	0.233	<u>0.249</u>	0.241	0.275	0.213	0.291	0.222	0.283	0.202	0.269	0.213	0.295	0.254	0.315
1 <sup>st</sup> Count		15	27	13	11	1	0	1	2	0	0	3	0	11	2	0	0	0	0

contrast, HGTS-Former abandons traditional HGNNs methods and instead leverages sparsity and transformer components to realize hypergraph aggregation. This design emphasizes fine-grained dynamic correlation modeling through a hierarchical hypergraph.

#### IV. EXPERIMENTS

##### A. Datasets and Evaluation Metric

We conducted experiments on eight datasets: ETTh1, ETTh2, ETTm1, ETTm2 [39], ECL [55], Traffic [55], Weather [55], and Solar-Energy [56]. (1) ETTh1 and ETTh2 are electricity datasets, containing 7 variables and sampled every hour. (2) ETTm1 and ETTm2 are electricity datasets, containing 7 variables and sampled every fifteen minutes. (3) ECL is an electricity dataset, containing 321 variables and sampled every hour. (4) Traffic is a transportation dataset, containing 862 variables and sampled every hour. (5) Weather is a climate dataset, containing 21 variables and sampled every ten minutes. (6) Solar-Energy is an energy dataset, containing 137 variables and sampled every ten minutes.

We choose Mean Square Error (MSE) and Mean Absolute Error (MAE) as our evaluation metrics, where lower values represent better performance.

##### B. Implementation Details

As shown in the Table II, we show the core hyperparameters in the training phase, where edge num is the number of

hyperedges in Intra-HyperGraph, it is worth noting that edge num must be greater than 3. This is because our hypergraph is sampled based on the confidence matrix by TOPK strategy, where  $TOPK = \lfloor \frac{edge\ num}{3} \rfloor$ . In addition, Inter-graph is generated according to the same strategy.  $P$  is the patch length, and  $L$  is the number of the layer. We utilize Adam as our optimizer. All experiments are implemented by Pytorch on a single A800 with 80GB of memory. More details can be found in our source code.

##### C. Comparison on Public Benchmark Datasets

• **Results on Long-term Forecasting Task.** Multivariate time series forecasting is crucial for predictive performance and decision-making value in complex real-world scenarios. Therefore, we train a single model on each dataset and use a rolling forecast approach (Lookback sequence length is 672) to evaluate it on four forecast steps of 96, 192, 336, and 720. It is worth noting that our method leverages an autoregressive method to predict the next token, so we only need to perform supervised training at a fine-grained level to predict arbitrary lengths adaptively.

The results in Table I demonstrate the superior performance of our model in multivariate time series forecasting. Our model performs well in 32 forecasting tasks on 8 widely used datasets. It achieved 15 firsts in MSE and 27 firsts in MAE, far exceeding other advanced models, reflecting its good generalization ability and accuracy. As the forecast

TABLE II: Experimental configurations of our proposed HGTS-Former, where lradj is the learning rate adjustment method

Experiment	Dataset	Configuration							Training Process			
		L	d_model	d_ff	H	P	edge num	lradj	LR	Loss	Batch Size	Epochs
Multivariate Forecasting	ETTh1	2	1024	2048	8	48	7	cosine	0.0001	MSE	32	10
	ETTh2	2	1024	2048	8	48	7	cosine	0.0001	MSE	32	10
	ETTh1	1	1024	2048	8	96	3	cosine	0.0001	MSE	32	10
	ETTh2	1	512	2048	8	96	3	cosine	0.0001	MSE	32	10
	ECL	4	512	2048	8	48	3	cosine	0.0001	MSE	8	10
	Traffic	4	512	2048	8	96	4	cosine	0.0002	MSE	4	10
	Weather	3	512	2048	8	96	4	cosine	0.0001	MSE	32	10
	Solar-Energy	2	1024	2048	8	48	8	cosine	0.0002	MSE	16	10
Imputation	ETTh1	2	256	1024	8	16	21	cosine	0.002	MSE	32	20
	ETTh2	1	256	1024	8	32	24	cosine	0.002	MSE	32	20
	ETTh1	2	256	1024	8	16	24	cosine	0.002	MSE	32	20
	ETTh2	1	256	1024	8	16	24	cosine	0.001	MSE	32	20
	ECL	2	256	512	8	16	24	cosine	0.0005	MSE	32	20
	Weather	1	256	1024	8	16	24	cosine	0.002	MSE	32	20

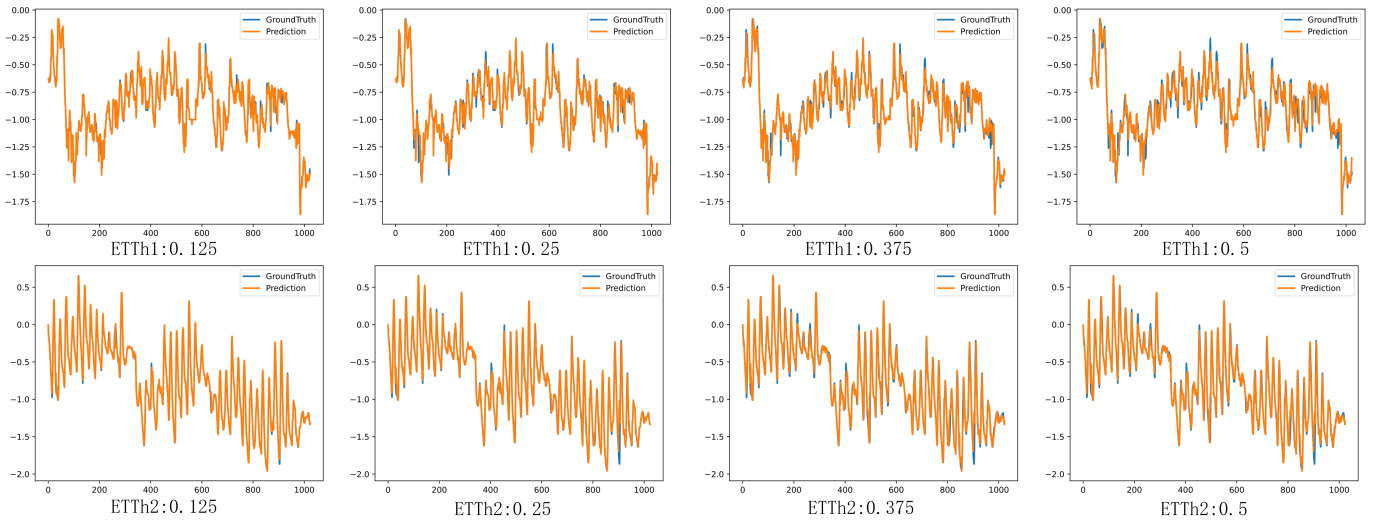


Fig. 3: Imputation result of our proposed model on the ETTh1 and ETTh2 datasets.

length increases, such as in tasks with forecast lengths of 336 and 720, the errors of most models increase significantly under long-term forecasts, while the performance of our model improves steadily, reflecting our model's excellent modeling ability in long-term dependencies.

• **Results on Imputation Task.** Accurately filling missing values is crucial in time series analysis, which directly affects the accuracy of model prediction results in practical applications.

Table III shows the performance of our model in filling missing values in time series on six different datasets. To evaluate our model, we randomly mask 12.5%, 25%, 37.5%, 50% of the time in a time series of length 1024, and the final result is the average of these 4 different masking rates. The MSE and MAE of our model are significantly lower than those of other advanced models, especially on ETTm1 and ETTh1, where our model consistently outperforms other models. Compared with the second-best performing model TimeMixer++ [57], our model reduces the MSE by 14.29% and MAE by 6.7% on average. In datasets with higher complexity (such as ETTm1, ETTm2, and ECL), the error of our model is much lower than that of other models, demonstrating its ability to capture complex time series patterns. At random masking ratios of

12.5% to 50%, our model can accurately predict different degrees of missing data, demonstrating the robustness of our model.

#### D. Component Analysis

In order to verify the effectiveness of each component of HGTS-Former, we conducted anomaly detection experiments on four datasets to evaluate the impact of different components on the overall performance. The full HGTS-Former model was used as the control group, and ablation experiments were performed by removing a single component (w/o). The results are shown in the Table IV. After removing MHSA and RoPE, the average MSE increased by 0.047 and the average MAE increased by 0.037, indicating the importance of MHSA and RoPE. MHSA and RoPE has the most obvious performance improvement. After removing IntraHGA, the average MSE increased by 0.013 and the average MAE increased by 0.006, indicating that IntraHGA is critical for modeling complex relationships between local variables and improves the performance of the model. After removing InterHGA, the average MSE increased by 0.011 and the average MAE increased by 0.007, indicating that the inter-group hypergraph

TABLE III: Full results of the imputation task across six datasets. To evaluate our model performance, we randomly mask {12.5%, 25%, 37.5%, 50% } of the time points in the time series of length 1024. The final results are averaged across these 4 different masking ratios.

	ETTh1		ETTh2		ECL		Weather	
	MSE	MAE	MSE	MAE	MSE	MAE	MSE	MAE
HGTS-Former (Ours)	<b>0.040</b>	<b>0.126</b>	<u>0.034</u>	<b>0.112</b>	<b>0.085</b>	<b>0.192</b>	<b>0.065</b>	<u>0.164</u>
TimeMixer++ (2025)	<u>0.041</u>	<u>0.127</u>	<b>0.024</b>	0.135	<u>0.091</u>	<u>0.198</u>	<b>0.065</b>	<b>0.157</b>
TimeMixer (2024b)	0.072	0.178	0.061	0.166	0.152	0.242	0.101	0.294
itransformer (2023)	0.075	0.177	0.055	0.169	0.130	0.213	0.125	0.259
PatchTST (2023)	0.097	0.194	0.080	0.183	0.178	0.231	0.124	0.293
Crossformer (2023)	0.081	0.196	0.111	0.219	0.201	0.309	0.206	0.308
FEDformer (2022b)	0.048	0.152	0.087	0.198	0.099	0.225	0.262	0.344
TIDE (2023a)	0.090	0.210	0.169	0.263	0.289	0.395	0.709	0.596
DLinear (2023)	0.076	0.191	0.088	0.198	0.174	0.288	0.120	0.238
TimesNet (2023)	0.049	0.147	0.035	<u>0.124</u>	0.142	0.258	<u>0.088</u>	0.198
MICN (2023a)	0.059	0.170	0.109	0.221	0.127	0.254	0.179	0.290

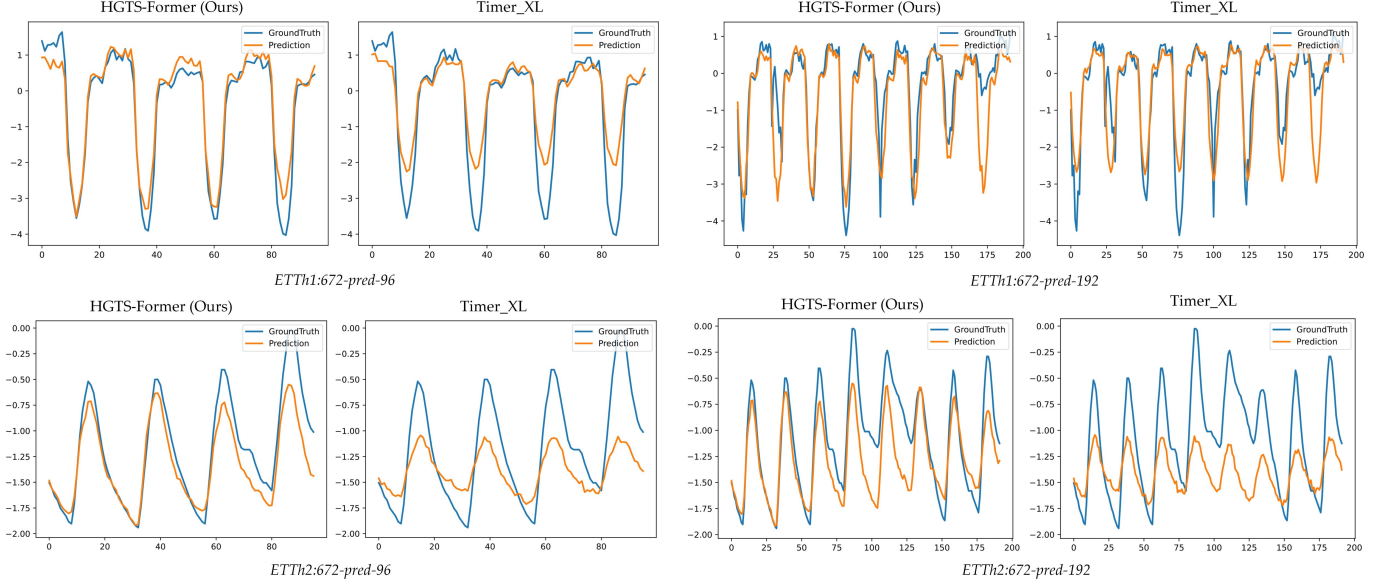


Fig. 4: Comparison of the predicted results between ours and Timer-XL on samples from the ETTh1 and ETTh2 datasets.

can model the interaction between different variable groups, proving the effectiveness of InterHGA. The experiments prove the rationality of the HGTS-Former structural design, and each component is indispensable.

#### E. Ablation Study

• **Results of Different Lookback Length.** We follow the TSF scaling law [58] to verify the impact of different input lengths on the results. As can be seen from Fig. 5(a), the model performance does not improve with increasing Lookback length. This may be because to ensure the effectiveness of Intra-HyperGraph construction, a short patch length is used when the length is short, resulting in incomplete temporal patterns and thus a decrease in performance.

• **Results of Different Parameter  $\alpha$ .** The purpose of the hyperparameter  $\alpha$  is to reduce the influence of non-hyperedge nodes on the aggregation process when performing numerical masking. As shown in Fig. 5(b), different  $\alpha$  does not have much impact on the performance of HGTS-Former, which shows that our model can well capture the potential temporal patterns within the variables and the dynamic relationship between variables.

• **Results of Different Backbone Blocks.** We verify the impact of the number of block layers on the experimental results on the ETTh1 dataset. As we can see from Fig. 5(c), the experimental results are getting better with the increase of the number of layers, which shows that the potential of our model has not been fully developed. It also further proves the effectiveness of our proposed method of using hierarchical



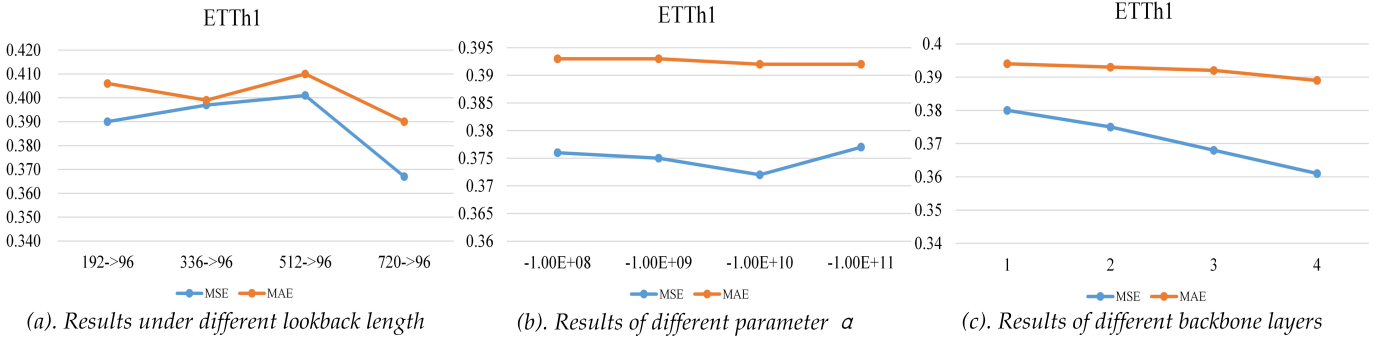


Fig. 5: Ablation study of different parameter configurations in our experiments.

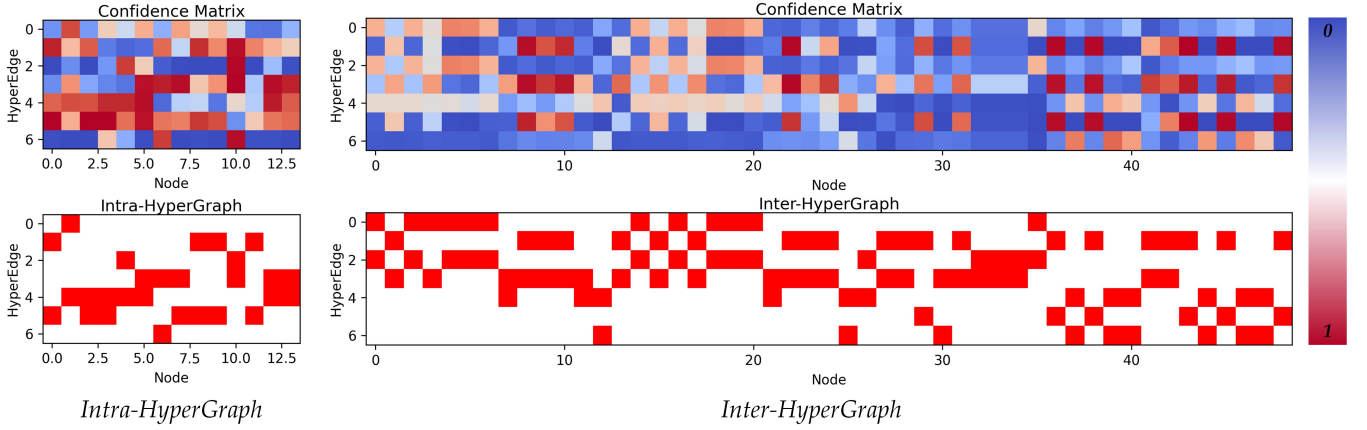


Fig. 6: Visualization of the Confidence Matrix and HyperGraph Visualization

TABLE IV: Component analysis of our proposed model on the ETT series datasets. *w/o* denotes without the corresponding component.

	ETTh1		ETTh2		ETTM1		ETTM2		Avg		Promotion	
	MSE	MAE	MSE	MAE	MSE	MAE	MSE	MAE	MSE	MAE	MSE	MAE
HGTS-Former	0.408	0.419	0.347	0.386	0.353	0.374	0.267	0.316	0.344	0.374	-	-
<i>w/o</i> MHSA+RoPE	0.449	0.457	0.405	0.427	0.395	0.409	0.316	0.350	0.391	0.411	<b>0.047</b>	<b>0.037</b>
<i>w/o</i> IntraHGA	0.411	0.417	0.357	0.388	0.371	0.386	0.287	0.328	0.357	0.380	<b>0.013</b>	<b>0.006</b>
<i>w/o</i> InterHGA	0.403	0.416	0.360	0.397	0.365	0.381	0.291	0.328	0.355	0.381	<b>0.011</b>	<b>0.007</b>

TABLE V: Efficiency analysis of HGTS-Former.

Metric	Parameter	Memory Usage	Speed
HGTS-Former	10.38M	738M	0.0133s/iter

hypergraphs to capture the potential temporal patterns within variables and the dynamic correlations between variables.

• **Efficiency Analysis & Model Parameters.** We analyze the efficiency of HGTS-Former during the training phase in Table V. Batch size is 4, L is 1,  $d_{\text{model}}$  is 512, and  $d_{\text{ff}}$  is 2048. The number of parameters of our model is 10.38M, the training speed is 0.0133s/iter, and the memory resources only occupy 738M.

#### F. Visualization

As shown in Fig. 6, we show the confidence matrix during the hierarchical hypergraph construction process and the com-

pleted hypergraph. HGTS-Former can effectively aggregate similar temporal patterns within variables and capture the dynamic correlation between different variables.

And we show the imputation results of ETTh1 and ETTh2 at different mask rates in Fig. 3. Thanks to the effective capture of temporal patterns within variables and relationships between variables by HGTS-Former, our method achieves SOTA performance on imputation tasks. This demonstrates the powerful capabilities of our model on other time series tasks.

As shown in Fig. 4, we show the prediction cases of HGTS-Former (ours) and Timer-XL [10] on 672-pred-96 and 672-pred-192. From Fig. 4, we can see that the performance of our model is better than that of Timer-XL [10]. Our model is better able to capture the temporal patterns when facing extreme changes. For example, in Fig. 4 ETTh1:672-pred-96, our model is closer to the ground truth when predicting extreme values.

## G. Limitation Analysis

As an autoregressive model, HGTS-Former will cause error accumulation when making long-term predictions. In addition, we have only explored the capabilities of HGTS-Former in long-term forecasting and imputation tasks, and further exploration is needed in other areas such as classification and anomaly detection

## V. CONCLUSION AND FUTURE WORKS

In this paper, we propose the patch-based HGTS-Former for time series tasks. By building a hierarchical hypergraph to aggregate the potential temporal patterns within variables and capture the group-wise dynamic correlations between variables, and the whole process is completed by transformer, overcoming the limitations of traditional hypergraph neural networks. We achieve SOTA performance on autoregressive forecasting and imputation tasks. Although HGTS-Former has excellent performance in long-term forecasting and imputation, its capabilities have not been fully explored in other downstream tasks. In the future, we will explore its capabilities in other time series tasks such as anomaly detection, short-term forecasting, and classification.

## REFERENCES

- [1] M. Wang, C. Wan, J. Lu, Z. Yu, B. Xiao, Y. Li, X. He, Z. Luo, Q. Yuan, Y. Hu *et al.*, "Time series extrinsic regression for reconstructing missing electron temperature in tokamak," *Nuclear Fusion*, vol. 65, no. 7, p. 076008, 2025.
- [2] S. Mehtab and J. Sen, "Stock price prediction using convolutional neural networks on a multivariate timeseries," *arXiv preprint arXiv:2001.09769*, 2020.
- [3] M. Jarrah and M. Derbali, "Predicting saudi stock market index by using multivariate time series based on deep learning," *Applied Sciences*, vol. 13, no. 14, p. 8356, 2023.
- [4] Z.-L. Xiang, R. Wang, X.-R. Yu, B. Li, and Y. Yu, "Experimental analysis of similarity measurements for multivariate time series and its application to the stock market," *Applied Intelligence*, vol. 53, no. 21, pp. 25 450–25 466, 2023.
- [5] W. Zheng and J. Hu, "Multivariate time series prediction based on temporal change information learning method," *IEEE Transactions on Neural Networks and Learning Systems*, vol. 34, no. 10, pp. 7034–7048, 2022.
- [6] M. U. Agada, "Multidimensional time series weather prediction using long short term memory neural network," Ph.D. dissertation, 2023.
- [7] L. Sanhudo, J. Rodrigues, and E. Vasconcelos Filho, "Multivariate time series clustering and forecasting for building energy analysis: Application to weather data quality control," *Journal of Building Engineering*, vol. 35, p. 101996, 2021.
- [8] Y. Liu, T. Hu, H. Zhang, H. Wu, S. Wang, L. Ma, and M. Long, "itransformer: Inverted transformers are effective for time series forecasting," *arXiv preprint arXiv:2310.06625*, 2023.
- [9] Y. Liu, H. Zhang, C. Li, X. Huang, J. Wang, and M. Long, "Timer: Generative pre-trained transformers are large time series models," *arXiv preprint arXiv:2402.02368*, 2024.
- [10] Y. Liu, G. Qin, X. Huang, J. Wang, and M. Long, "Timer-xl: Long-context transformers for unified time series forecasting," *arXiv preprint arXiv:2410.04803*, 2024.
- [11] X. Shi, S. Wang, Y. Nie, D. Li, Z. Ye, Q. Wen, and M. Jin, "Time-moe: Billion-scale time series foundation models with mixture of experts," *arXiv preprint arXiv:2409.16040*, 2024.
- [12] H. Zhang, Y. Liu, Y. Qiu, H. Liu, Z. Pei, J. Wang, and M. Long, "Timesbert: A bert-style foundation model for time series understanding," *arXiv preprint arXiv:2502.21245*, 2025.
- [13] Q. Huang, L. Shen, R. Zhang, S. Ding, B. Wang, Z. Zhou, and Y. Wang, "Crossgmn: Confronting noisy multivariate time series via cross interaction refinement," *Advances in Neural Information Processing Systems*, vol. 36, pp. 46 885–46 902, 2023.
- [14] Y. Hu, G. Zhang, P. Liu, D. Lan, N. Li, D. Cheng, T. Dai, S.-T. Xia, and S. Pan, "Timefilter: Patch-specific spatial-temporal graph filtration for time series forecasting," *arXiv preprint arXiv:2501.13041*, 2025.
- [15] Y. Luo, B. Zhang, Z. Liu, and Q. Ma, "Hi-patch: Hierarchical patch gnn for irregular multivariate time series," in *Forty-second International Conference on Machine Learning*.
- [16] Z. Shang and L. Chen, "Mshyper: Multi-scale hypergraph transformer for long-range time series forecasting," *arXiv preprint arXiv:2401.09261*, 2024.
- [17] Z. Shang, L. Chen, B. Wu, and D. Cui, "Ada-mshyper: adaptive multi-scale hypergraph transformer for time series forecasting," *Advances in Neural Information Processing Systems*, vol. 37, pp. 33 310–33 337, 2024.
- [18] B. Li, Y. Luo, Z. Liu, J. Zheng, J. Lv, and Q. Ma, "Hyperimts: Hypergraph neural network for irregular multivariate time series forecasting," *arXiv preprint arXiv:2505.17431*, 2025.
- [19] X. Wang, G. Chen, G. Qian, P. Gao, X.-Y. Wei, Y. Wang, Y. Tian, and W. Gao, "Large-scale multi-modal pre-trained models: A comprehensive survey," *Machine Intelligence Research*, vol. 20, no. 4, pp. 447–482, 2023.
- [20] A. Vaswani, N. Shazeer, N. Parmar, J. Uszkoreit, L. Jones, A. N. Gomez, Ł. Kaiser, and I. Polosukhin, "Attention is all you need," *Advances in neural information processing systems*, vol. 30, 2017.
- [21] X. Wang, J. Li, L. Zhu, Z. Zhang, Z. Chen, X. Li, Y. Wang, Y. Tian, and F. Wu, "Visevent: Reliable object tracking via collaboration of frame and event flows," *IEEE Transactions on Cybernetics*, vol. 54, no. 3, pp. 1997–2010, 2023.
- [22] X. Wang, S. Wang, C. Tang, L. Zhu, B. Jiang, Y. Tian, and J. Tang, "Event stream-based visual object tracking: A high-resolution benchmark dataset and a novel baseline," in *Proceedings of the IEEE/CVF Conference on Computer Vision and Pattern Recognition*, 2024, pp. 19 248–19 257.
- [23] X. Wang, Y. Rong, Z. Wu, L. Zhu, B. Jiang, J. Tang, and Y. Tian, "Sstformer: Bridging spiking neural network and memory support transformer for frame-event based recognition," *IEEE Transactions on Cognitive and Developmental Systems*, 2025.
- [24] X. Wang, J. Jin, C. Li, J. Tang, C. Zhang, and W. Wang, "Pedestrian attribute recognition via clip-based prompt vision-language fusion," *IEEE Transactions on Circuits and Systems for Video Technology*, vol. 35, no. 1, pp. 148–161, 2025.
- [25] J. Devlin, M.-W. Chang, K. Lee, and K. Toutanova, "Bert: Pre-training of deep bidirectional transformers for language understanding," in *Proceedings of the 2019 conference of the North American chapter of the association for computational linguistics: human language technologies, volume 1 (long and short papers)*, 2019, pp. 4171–4186.
- [26] A. Dosovitskiy, L. Beyer, A. Kolesnikov, D. Weissenborn, X. Zhai, T. Unterthiner, M. Dehghani, M. Minderer, G. Heigold, S. Gelly *et al.*, "An image is worth 16x16 words: Transformers for image recognition at scale," *arXiv preprint arXiv:2010.11929*, 2020.
- [27] Y. Nie, N. H. Nguyen, P. Sinthong, and J. Kalagnanam, "A time series is worth 64 words: Long-term forecasting with transformers," *arXiv preprint arXiv:2211.14730*, 2022.
- [28] S. Li, X. Jin, Y. Xuan, X. Zhou, W. Chen, Y.-X. Wang, and X. Yan, "Enhancing the locality and breaking the memory bottleneck of transformer on time series forecasting," *Advances in neural information processing systems*, vol. 32, 2019.
- [29] B. Lim, S. Ö. Arık, N. Loeff, and T. Pfister, "Temporal fusion transformers for interpretable multi-horizon time series forecasting," *International journal of forecasting*, vol. 37, no. 4, pp. 1748–1764, 2021.
- [30] T. Zhou, Z. Ma, Q. Wen, X. Wang, L. Sun, and R. Jin, "Fedformer: Frequency enhanced decomposed transformer for long-term series forecasting," in *International conference on machine learning*. PMLR, 2022, pp. 27 268–27 286.
- [31] S. Liu, H. Yu, C. Liao, J. Li, W. Lin, A. X. Liu, and S. Dustdar, "Pyraformer: Low-complexity pyramidal attention for long-range time series modeling and forecasting," in *# PLACEHOLDER\_PARENT\_METADATA\_VALUE#*, 2022.
- [32] A. Das, W. Kong, R. Sen, and Y. Zhou, "A decoder-only foundation model for time-series forecasting," in *Forty-first International Conference on Machine Learning*, 2024.
- [33] G. Woo, C. Liu, A. Kumar, C. Xiong, S. Savarese, and D. Sahoo, "Unified training of universal time series forecasting transformers," 2024.
- [34] A. F. Ansari, L. Stella, C. Turkmen, X. Zhang, P. Mercado, H. Shen, O. Shchur, S. S. Rangapuram, S. P. Arango, S. Kapoor *et al.*, "Chronos: Learning the language of time series," *arXiv preprint arXiv:2403.07815*, 2024.

- [35] B. K. Nelson, "Time series analysis using autoregressive integrated moving average (arima) models," *Academic emergency medicine*, vol. 5, no. 7, pp. 739–744, 1998.
- [36] G. P. Zhang, "Time series forecasting using a hybrid arima and neural network model," *Neurocomputing*, vol. 50, pp. 159–175, 2003.
- [37] L. Wang, H. Zou, J. Su, L. Li, and S. Chaudhry, "An arima-ann hybrid model for time series forecasting," *Systems Research and Behavioral Science*, vol. 30, no. 3, pp. 244–259, 2013.
- [38] S. Bhanja and A. Das, "Deep neural network for multivariate time-series forecasting," in *Proceedings of International Conference on Frontiers in Computing and Systems: COMSYS 2020*. Springer, 2020, pp. 267–277.
- [39] A. Zeng, M. Chen, L. Zhang, and Q. Xu, "Are transformers effective for time series forecasting?" in *Proceedings of the AAAI conference on artificial intelligence*, vol. 37, no. 9, 2023, pp. 11 121–11 128.
- [40] T. Dai, B. Wu, P. Liu, N. Li, J. Bao, Y. Jiang, and S.-T. Xia, "Periodicity decoupling framework for long-term series forecasting," in *The Twelfth International Conference on Learning Representations*, 2024.
- [41] Y. Zhang and J. Yan, "Crossformer: Transformer utilizing cross-dimension dependency for multivariate time series forecasting," in *The eleventh international conference on learning representations*, 2023.
- [42] G. Yu, J. Zou, X. Hu, A. I. Aviles-Rivero, J. Qin, and S. Wang, "Revitalizing multivariate time series forecasting: Learnable decomposition with inter-series dependencies and intra-series variations modeling," *arXiv preprint arXiv:2402.12694*, 2024.
- [43] J. Chen, J. E. Lenssen, A. Feng, W. Hu, M. Fey, L. Tassioulas, J. Leskovec, and R. Ying, "From similarity to superiority: Channel clustering for time series forecasting," *Advances in Neural Information Processing Systems*, vol. 37, pp. 130 635–130 663, 2024.
- [44] X. Qiu, X. Wu, Y. Lin, C. Guo, J. Hu, and B. Yang, "Duet: Dual clustering enhanced multivariate time series forecasting," *arXiv preprint arXiv:2412.10859*, 2024.
- [45] J. Liu, M. Cao, and S. Chen, "Timecheat: A channel harmony strategy for irregularly sampled multivariate time series analysis," in *Proceedings of the AAAI Conference on Artificial Intelligence*, vol. 39, no. 18, 2025, pp. 18 861–18 869.
- [46] Y. Huang, Q. Liu, and D. Metaxas, "Video object segmentation by hypergraph cut," in *2009 IEEE conference on computer vision and pattern recognition*. IEEE, 2009, pp. 1738–1745.
- [47] R. Sawhney, S. Agarwal, A. Wadhwa, T. Derr, and R. R. Shah, "Stock selection via spatiotemporal hypergraph attention network: A learning to rank approach," in *Proceedings of the AAAI Conference on Artificial Intelligence*, vol. 35, no. 1, 2021, pp. 497–504.
- [48] C. Xu, M. Li, Z. Ni, Y. Zhang, and S. Chen, "Groupnet: Multiscale hypergraph neural networks for trajectory prediction with relational reasoning," in *Proceedings of the IEEE/CVF Conference on Computer Vision and Pattern Recognition*, 2022, pp. 6498–6507.
- [49] N. Yadati, M. Nimishakavi, P. Yadav, V. Nitin, A. Louis, and P. Talukdar, "Hypergen: A new method for training graph convolutional networks on hypergraphs," *Advances in neural information processing systems*, vol. 32, 2019.
- [50] Y. Feng, H. You, Z. Zhang, R. Ji, and Y. Gao, "Hypergraph neural networks," in *Proceedings of the AAAI conference on artificial intelligence*, vol. 33, no. 01, 2019, pp. 3558–3565.
- [51] J. Su, M. Ahmed, Y. Lu, S. Pan, W. Bo, and Y. Liu, "Roformer: Enhanced transformer with rotary position embedding," *Neurocomputing*, vol. 568, p. 127063, 2024.
- [52] J. Fixelle, "Hypergraph vision transformers: Images are more than nodes, more than edges," in *Proceedings of the Computer Vision and Pattern Recognition Conference*, 2025, pp. 9751–9761.
- [53] S. Lin, H. Chen, H. Wu, C. Qiu, and W. Lin, "Temporal query network for efficient multivariate time series forecasting," *arXiv preprint arXiv:2505.12917*, 2025.
- [54] C. Tian, Z. Lu, Z. Zhang, H. Yang, W. Cao, Z. Guo, X. Sun, and L. Jin, "Hypermixer: Specializable hypergraph channel mixing for long-term multivariate time series forecasting," in *Proceedings of the AAAI Conference on Artificial Intelligence*, vol. 39, no. 19, 2025, pp. 20 885–20 893.
- [55] H. Wu, J. Xu, J. Wang, and M. Long, "Autoformer: Decomposition transformers with auto-correlation for long-term series forecasting," *Advances in neural information processing systems*, vol. 34, pp. 22 419–22 430, 2021.
- [56] G. Lai, W.-C. Chang, Y. Yang, and H. Liu, "Modeling long-and short-term temporal patterns with deep neural networks," in *The 41st international ACM SIGIR conference on research & development in information retrieval*, 2018, pp. 95–104.
- [57] S. Wang, J. Li, X. Shi, Z. Ye, B. Mo, W. Lin, S. Ju, Z. Chu, and M. Jin, "Timemixer++: A general time series pattern machine for universal predictive analysis," *arXiv preprint arXiv:2410.16032*, 2024.
- [58] J. Shi, Q. Ma, H. Ma, and L. Li, "Scaling law for time series forecasting," *Advances in Neural Information Processing Systems*, vol. 37, pp. 83 314–83 344, 2024.